Proceeding of the IEEE
International Conference on Robotics and Biomimetics
Dali, China, December 2019

Online Center of Mass Detection for Quadruped Robots in Trot Gait Motion*

Chao Ding[1], Lelai Zhou[1], Xuewen Rong[1] and Yibin Li[1]

***Abstract*— Most of the motion control strategies for the quadruped robots are based on the trajectory planning of the center of mass (CoM) and the hypothesis that the CoM locates at the geometrical center of the trunk. In fact, the CoM position offsets will introduce obvious influence to the control performance. This paper presents a method for online CoM detection for quadruped robots running in trot gait. The dynamical model of the robot is built in the inertial coordinate system. Transforming methods for the status variables from the base frame to the inertial frame are also provided. To get more precise results, the step height compensation method for swing feet and comparative ground reaction force calculations are presented. With the proposed method, the analytical solution of the CoM position is obtained. Simulations show the effectiveness of the proposed method.**

I. INTRODUCTION

In the last ten years, legged robots have been widely studied in the area of bionic robotics. Quadruped robots begin to arise since the appearance of BigDog [1], a platform released by the Boston Dynamics company, aiming at the mobile equipment support for individual combat. From then on, various quadruped robots and humanoid robots appear. The main applications of these robots are payload transportation, maneuvering on rough terrain [2] [3], industrial manufacture, and home service [4].

For humanoid robots, in order to prevent tumbling, it is very important to maintain the center of mass (CoM) locating at the middle of the two feet. Therefore, at the beginning of the humanoid research, the feet usually had exaggerated large size to achieve this so that robots could have larger stability margin. With the advance of the control methods, the CoM can be detected more precisely and the humanoids ran more flexibly. The classical ZMP-based (zero moment point) control method is a production of this thought.

For quadruped robots, the quadrangle surrounded by their four feet provides more stability margin. So, they have larger fault tolerance for the offset between the CoM and the geometrical center. Besides, in the mechanical design process, the components are distributed as uniformly as possible. Most controllers for quadruped robots regard the geometrical center as the CoM, and make motion control decisions based on this assumption.

*This work is funded by the National Key R&D Program of China (Grand No. 2017YFC0806505), the National Natural Science Foundation of China (Grand No. U1613223 and 61973191), and the National High Technology Research and Development Program of China (Grand No. 2015AA042201).

[1]Authors are with the Center for Robotics, School of Control Science and Engineering, Shandong University, China, corresponding author: Lelai Zhou email: zhoulelai@sdu.edu.cn

In fact, through a mass of experiments on our quadruped prototype, we found that even a small error between the CoM and the trunk center could introduce macroscopic instability to the robot [5]. Benjamin [6] also proved that the unknown modelling errors, such as the CoM measurement offset resulted in inaccurate state estimates. In the case of position control based on fixed trajectory planning, the unexpected rotations could introduce unexpected feet bounding/sliding and drastic orientation oscillation to the robot [7]. When the compliance method was applied, the performance became a little better. In the case of virtual leg model based force control architecture, the orientation of the trunk could maintain nearly ideal, but the extra gravitational moment would introduce unanticipated lateral and longitudinal velocities [8]. When the robot was walking in static gait, this error brought serious interference to the judgement of the stability margin and even caused tumbling [9] [10].

Besides, the robot controllers conventionally regarded the CoM as a fixed point that would not drift in the whole movement process, which resulted in a strong dependence on the CoM position accuracy [11]. In fact, as a transportation platform, the CoM of the quadruped robots shifted whenever the payloads changed. It was strongly necessary to detect the real CoM of the quadruped robot in real time so that the controller could take corresponding compensatory measures in time.

Recently, there were some improvements in the control methods that could tolerate tiny CoM offsets to some extent. Tomislav [12] proposed a model predictive control (MPC) based control architecture for quadruped robots in which the estimated CoM could converge to the true value.

Some researchers have studied the methods of the CoM position detection. Giovanni [13] presented a strategy for effective CoM calculation with two force sensors on the robot feet. Hamidreza [14] designed an estimator based on Kalman Filter to estimate the CoM position and velocity of the humanoid robot. But this method failed when applied to faster motions. SangJoo [15] proposed a closed-loop observer based on the inverted pendulum model to get more precise estimation of the CoM even with parametric uncertainties and external disturbances. Michele [16] discussed a method to identify the position of CoM with static pose. Guido [17] improved it and proposed a recursive method for online identification of the CoM position based on the orientation error and contact forces. This method was activated whenever the payload changes but the robot needed to stop immediately to obtain enough pose and force data sets and wait until the adjustments were finished.

978-1-7281-6321-5/19//$31.00 ©2019 IEEE

The main contribution of this paper is a CoM detection method for quadruped robots to identify the current CoM position incessantly while running in trot gait. This paper also proposes the observation methods for the crucial robot states that are used in the dynamic model. The state-of-art methods usually divide the CoM detection approach into two steps: firstly the robots detect the changes of the CoM position mainly based on the leg forces or the attitudes, then the robots stop to adjust the settings and resume the movements after the adjustments. Besides, these methods are mainly applied in the static walk gait. The highlight of this work lies in that the proposed method can identify the CoM position at the beginning of the dynamic trot gait. This inspires us to run the detections and adjustments concurrently through every servo cycles. The primary identification results can be used to improve the attitude control performance and the more upright attitude can then make the CoM detection more precise.

This paper is organized as follows. Section I introduces the necessity of this work and gives an overview of the related researches. Section II builds the kinematic model and the dynamic model of the quadruped robot in trot gait, and presents the method for CoM estimation. Section III compared two different methods for ground reaction force (GRF) acquirement. Section IV shows the simulation results of the proposed method. Section V gives the conclusion.

II. DETECTION OF CoM POSITION IN TROT GAIT

The quadruped robot Scalf-II is designed to be a mobile platform to perform industrial, rescue, and transportation tasks, as shown in Fig. 1. The four legs distribute symmetrically about the geometric center of the trunk with all the knee joints pointing to the outer side of the trunk. It is powered by a gasoline engine and actuated by twelve hydraulic cylinders. Control strategies of its motions are finally achieved through the control of the electro-hydraulic servo valves on the cylinders.

A. Kinematic Model of the Legs

Since the four legs are symmetrical with the same structure, the topological structure and parameters of only one leg is shown in Fig. 2 representatively.

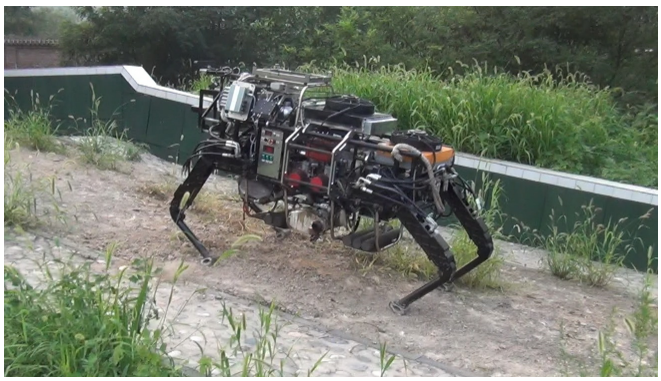

Fig. 1. Prototype of the quadruped robot Scalf-II.

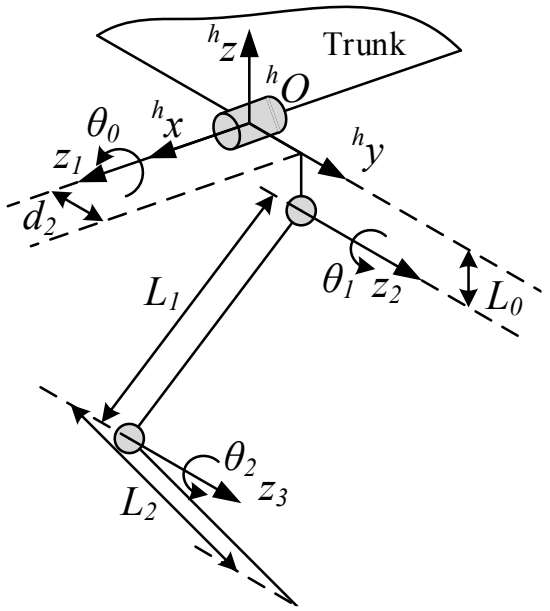

Fig. 2. Topological structure and main parameters of one leg. θ_0, θ_1 and θ_2 are the joint variables. $\{o_h\}$ is the base coordinates locates on the hip and fixed on the trunk.

The kinematic model of this leg can be written as:

$$^hp = \begin{bmatrix} ^hx \\ ^hy \\ ^hz \end{bmatrix} = \begin{bmatrix} -L_1 s_1 - L_2 s_{12} \\ L_0 s_0 + L_1 s_0 c_1 + L_2 s_0 c_{12} + \lambda d_2 c_0 \\ -L_0 c_0 - L_1 c_0 c_1 - L_2 c_0 c_{12} + \lambda d_2 s_0 \end{bmatrix} \quad (1)$$

where $s_i = sin\theta_i, c_i = cos\theta_i, i, j = \{0,1,2\}, s_{12} = sin(\theta_1 + \theta_2), c_{12} = cos(\theta_1 + \theta_2)$, the value of λ is 1 when applied to the left legs, and -1 to the right ones, $^hp = [^hx, ^hy, ^hz]^T$ is the foot position in $\{o_h\}$.

The Jacobian of this leg can be obtained as:

$$J(\theta) = \begin{bmatrix} 0 & -L_1 c_1 - L_2 c_{12} & -L_2 c_{12} \\ L_0 c_0 + L_1 c_0 c_1 + L_2 c_0 c_{12} - \lambda d_2 s_0 & -L_1 s_0 s_1 - L_2 s_0 s_{12} & -L_2 s_0 s_{12} \\ L_0 s_0 + L_1 s_0 c_1 + L_2 s_0 c_{12} + \lambda d_2 c_0 & L_1 c_0 s_1 + L_2 c_0 s_{12} & L_2 c_0 s_{12} \end{bmatrix}^T \quad (2)$$

B. Dynamic Model of the Robot in Trot Gait

The most commonly used gait of the quadruped robot for marching is the trot gait. On the condition of the duty factor of 0.5, the robot has two legs in the standing phase in the diagonal direction, while the other two legs in the swing phase, at any time. These two pairs of legs execute motions synchronously and has a phase difference of π. Under ideal conditions, the CoM locates at the geometrical center of the trunk, so that the robot will not rotate about the axis which is defined by the two feet of the standing legs.

In fact, the position of the CoM of the prototype hardly coincides with the geometrical center of the trunk. When there are some offsets between the real CoM and the trunk center, the gravity force of the trunk will exert torques that will drive the robot to rotate about the diagonal line of the standing feet, illustrated as the x_g-axis in Fig. 3. For our prototype, when the horizontal distance from the CoM

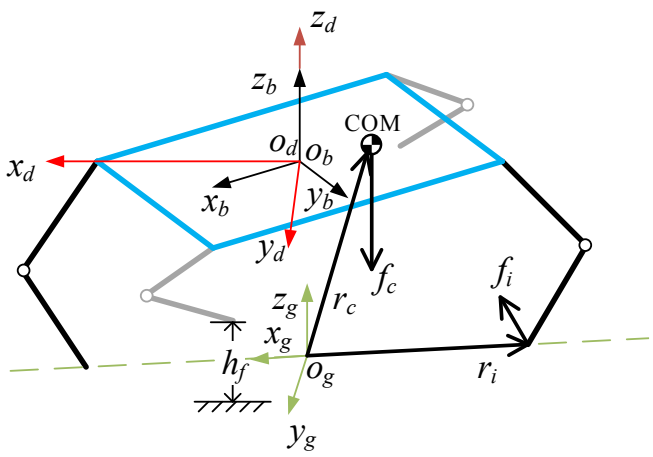

Fig. 3. Dynamic model of the robot when it is running in trot gait.

and the x_g-axis is only 5cm, the angular moment of gravity force about this axis can reach up to 150 N·m. Since the interaction forces between the feet and the ground cannot contribute effective moments around this axis, this rotation is uncontrollable.

When the quadruped robot is running in trot gait, there are two kinds of forces acting on it: the contact forces between the standing feet and the ground, and the gravity. In this work, the dynamic model of the robot is built in the inertial frame $\{o_g\}$, as shown in Fig. 3. The origin of $\{o_g\}$ locates at the middle of the standing feet with the x_g-axis pointing to the front leg and the z_g-axis vertically upward. Based on the Euler dynamics, the motion of the robot can be expressed by the following equation:

$$\sum_i (r_i \times f_i) + r_c \times f_c = {}^g I\, {}^g\dot{\omega} + {}^g\omega \times ({}^g I\, {}^g\omega) \tag{3}$$

where $f_i \in \boldsymbol{R}^3$ is the reactive force received by the standing feet from the ground, $f_c \in \boldsymbol{R}^3$ the gravity, $r_i \in \boldsymbol{R}^3$ and $r_c \in \boldsymbol{R}^3$ the corresponding lever arms with respect to the origin o_g, ${}^g I$ the inertial tensor and ${}^g\omega$ the angular velocity. The four legs are respectively named as the right front (RF) leg, the left front (LF) leg, the right hind (RH) leg and the left hind (LH) leg. $i \in \{RF, LF, RH, LH\}$.

Since the kinematics and Jacobian in Section II-A is based on the hip frame, the position of the foot in the base frame can be easily obtained as:

$${}^b p_i = \begin{bmatrix} {}^b x_i & {}^b y_i & {}^b z_i \end{bmatrix}^T = {}^h p_i + {}^b p_h \tag{4}$$

where ${}^b p_h$ is a position vector that is determined by the width W and the length L of the trunk.

The inertial measurement unit (IMU) is mounted in the diagonal frame $\{o_d\}$, which has the consistent origin and z-axis with the base frame $\{o_b\}$ and x_d-axis connecting the diagonal hips of the standing legs. So, the foot position and foot force in $\{o_d\}$ is:

$${}^d p_i = {}^d_b R\, {}^b p_i = R(z_b, \alpha)\, {}^b p_i \tag{5}$$

$${}^d f_i = R(z_b, \alpha)\, {}^b f_i \tag{6}$$

where ${}^b f_i$ is foot force in the base frame, α is the rotate angle from x_b-axis to x_b-axis around z_b-axis and $|\alpha| = arctan(W/L)$.

When the roll angle and the pitch angle are not too large, the angular velocity in the inertial frame - ${}^g\omega$ and the angular velocity measured by the IMU - ${}^d\omega$ have the following relationship:

$${}^g\omega = R(z_g, \varphi)\, {}^d\omega \tag{7}$$

where φ is the angle from x_g-axis to x_d-axis around z_g-axis, and can be got from the foot position:

$$\varphi = arctan \frac{{}^d y_h - {}^d y_f}{{}^d x_f - {}^d x_h} \tag{8}$$

with ${}^d p_f = [{}^d x_f, {}^d y_f, {}^d z_f]^T$ and ${}^d p_h = [{}^d x_h, {}^d y_h, {}^d z_h]^T$ respectively the position of the front and the hind feet in $\{o_d\}$.

Inherently the attitude angles measured by IMU module are Tait-Bryan angles which are commonly referred to as the y–z'–x'' intrinsic rotations. Based on the correspondence between the two coordinate systems, the rotation from $\{o_g\}$ to $\{o_d\}$ is:

$${}^g_d R = R(z_d, \varphi) R(y_d, \theta) R(x_d, \phi) \tag{9}$$

where $\Theta = [\phi, \theta, \varphi]^T$ is the pseudo attitude angle. ϕ and θ are the pitch and roll angles measured by the IMU. φ is the pseudo yaw angle defined by (8).

Based on the rotations above, the reactive forces received by the standing feet can be obtained as:

$$f_i = -{}^g f_i = -{}^g_d R\, {}^d f_i \tag{10}$$

where ${}^g f_i$ is the force thrust to the ground.

Since the dynamic model is built in the inertial system, the inertia tensor of the robot is a time-varying matrix. It varies with the variation of the position and the orientation of the trunk. The mass of the legs is neglected in this work since it is pretty small comparing to the mass of the trunk. Usually, the trunk maintains nearly horizontal ($\phi \approx 0, \theta \approx 0$) when running on the flat terrain. When there are few twist motions in the hip adduction/abduction joints, the inertia tensor can be approximately calculated as:

$${}^g I = {}^d I + m({}^g p_d{}^T\, {}^g p_d I_3 - {}^g p_d\, {}^g p_d{}^T) \tag{11}$$

where ${}^d I$ is the constant inertia tensor in the diagonal frame and can be calculated by integration or obtained directly from the computer-aided design (CAD) software. ${}^g p_d = [{}^g x_d, {}^g y_d, {}^g z_d]^T$ is the position of o_d in $\{o_g\}$, which can be estimated by the foot position:

$${}^g p_d = \begin{bmatrix} -\frac{1}{2}({}^d x_f + {}^d x_h) cos\theta - \frac{1}{2}({}^d z_f + {}^d z_h) sin\theta \\ -\frac{1}{2}({}^d y_f + {}^d y_h) cos\phi + \frac{1}{2}({}^d z_f + {}^d z_h) sin\phi \\ -\frac{1}{2}({}^d z_f + {}^d z_h) cos\phi \end{bmatrix} \tag{12}$$

Similarly, the lever arms of the ground reaction forces can be expressed as:

$${}^g r_h = -{}^g r_f = \begin{bmatrix} ({}^d x_f - {}^d x_h)/2/cos\varphi \\ 0 \\ 0 \end{bmatrix} \tag{13}$$

The level arm of the gravity is:

$$r_c = {}^g p_c = {}^g p_d + {}^g_d R \, {}^d_b R \, {}^b p_c \tag{14}$$

where ${}^b p_c = [x_c, y_c, 0]^T$ is the real CoM position in the base frame. When the CoM offset in the vertical direction is not too large, its effects on the motion performance on flat terrain are not obvious. So, in this work, we only take x_c and y_c in to consideration.

C. Analytical solution of the CoM position

With the calculations and transformations above, the dynamic model (3) can be simplified to the following form:

$$\begin{aligned} &\begin{bmatrix} -{}^g_d r_{21} & -{}^g_d r_{22} \\ {}^g_d r_{11} & {}^g_d r_{12} \\ \hdashline 0 & 0 \end{bmatrix} \begin{bmatrix} x_c \\ y_c \end{bmatrix} = \frac{K(q,\dot{q},\ddot{q})}{mg} - G(q) \\ &= H(q,\dot{q},\ddot{q}) = \begin{bmatrix} h_1(q,\dot{q},\ddot{q}) \\ h_2(q,\dot{q},\ddot{q}) \\ \hdashline h_3(q,\dot{q},\ddot{q}) \end{bmatrix} \end{aligned} \tag{15}$$

where $K(q,\dot{q},\ddot{q}) = {}^g I \, {}^g\dot{\omega} + {}^g\omega \times ({}^g I \, {}^g\omega) - \sum_i (r_i \times f_i)$, $G(q) = [-{}^g y_d, {}^g x_d, 0]^T$, ${}^g_d r_{ij}$ are the elements of ${}^g_d R$, $(q,\dot{q},\ddot{q})$ the attitude angle, angular velocity and angular acceleration, and m is the mass of the trunk.

Rewrite the first two lines of (15), we can get:

$$R'(q) p_{x,y} = H'(q,\dot{q},\ddot{q}) \tag{16}$$

In (16), $R'(q) \in \boldsymbol{R}^2$ is usually a non-singular matrix. So, the analytical solution of the CoM position can be expressed as:

$$p_{x,y} = R'^{-1}(q) H'(q,\dot{q},\ddot{q}) \tag{17}$$

D. Vertical Step Height Compensation of the Swing Feet

To get more convincing observations of the robot states $[\Theta, \dot{\Theta}, \ddot{\Theta}]^T$, in this work, the controller for motion planning of the quadruped robot legs is a position servo system that strictly follows the pre-defined foot trajectory. With this controller, there are more significant trunk rotations about x_g-axis. However, this controller will introduce obvious errors to the vertical step height h_f of the swing feet, as shown in Fig. 3, resulting in asynchronous phases of the diagonal legs. It will cause violent oscillations of the trunk orientation at the moment of foot phase switches.

In addition, (11) is obtained under the assumption that the body coordinate system is approximately parallel to the inertial frame. The proposed method becomes inaccuracy when the attitude angles are too large. To balance the conflicts between the different requirements, a compensation approach for the vertical step height is applied.

Similar to the rotations of coordinates in (9), the position of the swing foot in $\{o_g\}$ can be regarded as a map of that in $\{o_b\}$ after a series of rotations and translations from the hypothetical position in which the robot is horizontal. That is:

$${}^g p_i = {}^g p_b + R(z_b, {}^b\varphi) R(y_b, {}^b\theta) R(x_b, {}^b\phi) \, {}^b p_i \tag{18}$$

where ${}^b\Theta = [{}^b\phi, {}^b\theta, {}^b\varphi]^T$ is the attitude angle vector in the base frame, ${}^g p_b$ equals to ${}^g p_d$ in (12).

Marking the desired vertical step height of swing leg as ${}^g h_{i,d}$, the compensated desired position of the swing foot in the hip base frame can be obtained as:

$${}^h z_i = \frac{-H_t + {}^g h_{i,d} + ({}^h x_i + 0.5L) s^b\phi - ({}^h y_i + 0.5W) c^b\theta \, s^b\phi}{c^b\phi \, c^b\theta} \tag{19}$$

where H_t is the standing height of the trunk and is usually set to be a constant. $s^b\phi$, $c^b\phi$ and $c^b\theta$ stand for $sin^b\phi$, $cos^b\phi$ and $cos^b\theta$ respectively. For more precise control performance, it can be adjusted by the feedback position of the standing feet. H_t is also the z component of ${}^g p_b$.

Equation (19) is valid for the RF leg when it is in the swing phase. For the other three legs, it differs only in the sign of the terms $0.5L$ and $0.5W$.

III. ESTIMATION OF THE GROUND REACTION FORCE

In this work, two methods for the ground reaction force (GRF) estimation are tested.

Four 3d-force sensors are mounted at the end of each leg, as the red spherical objects shown in Fig. 4. The simulator returns a 3d-vector of GRFs expressed in the coordinate system of the force sensor - ${}^s f_i$. With the rotation matrix from the sensor frame to the base frame, the foot force can be obtained as:

$${}^b f_i = -{}^b_s R \, {}^s f_i \tag{20}$$

In this way, we intend to get the GRFs directly and reduce the computational cost. But in the simulations, huge errors appear in the CoM detection results.

To verify the validity of the force sensors, another four sensors fixed to the ground are add to the simulator corresponding to each foot. These sensors can detect the true force values exerted to the ground.

For comparision, another method for force estimation based on joint torques and the Jacobian in Section II-A is introduced:

$${}^b f_i = J^{-T}(\theta) \tau \tag{21}$$

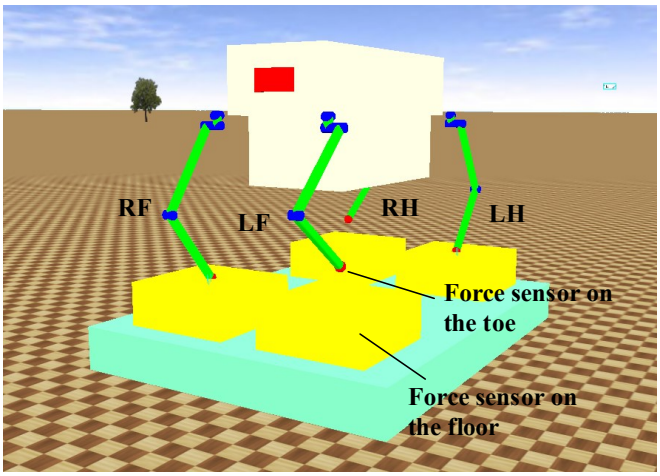

Fig. 4. Whole robot model and the estimation of ground reaction force.

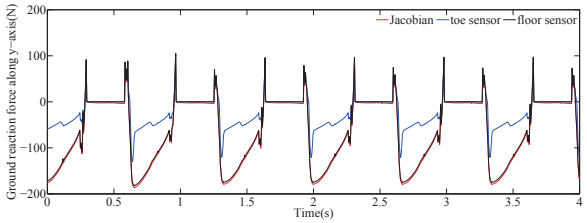

(a) GRF along x-axis

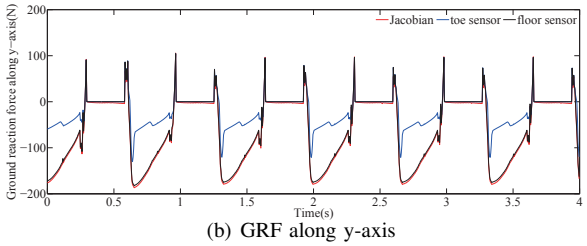

(b) GRF along y-axis

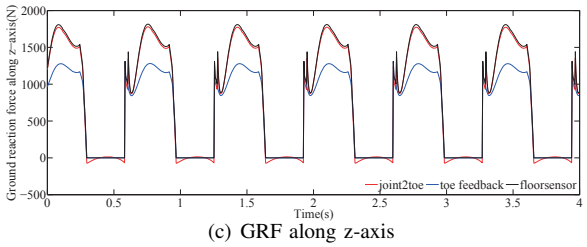

(c) GRF along z-axis

Fig. 5. GRF detection results with different approaches

The comparative simulation results of GRFs with different approaches are shown in Fig. 5. The red line corresponds to the force calculated using the Jacobian, the blue line corresponds to that using the force sensors mounted in the toe, and the black line is the value detected by the sensors mounted on the floor.

It is obvious that the method of (20) returns the GRF values with errors that can reach the scale of up to 50% of the true values, while the results of (21) follow the true values quite precisely.

This happens because of the internal mechanism of the force sensor modules in the simulator. The sensor returns the cumulative forces currently applied to its body, while the interaction between the foot and the ground is a complicated procedure. The sensors is highly influenced by its materials and the installation styles.

IV. RESULTS AND DISCUSSIONS

Simulations are executed in the software Webots Pro 2018a - a robot simulator providing a complete development environment for mobile robots. Main structure parameters and motion parameters are listed in Table I.

In Webots, the center of mass of a physical solid can be configured manually by the users. In order to simulate the offsets of CoM in the $x_b - y_b$ plane, three different reference offset values for $p_{x,y}$ were set into the model in this work: $\Delta x_c = \{0cm, -3cm, -10cm\}$, $\Delta y_c = \{0cm, 3cm, 10cm\}$.

After the CoM offsets were given to the model, the robot was ordered to step in situ in trot gait. The estimated CoM positions of the robot under different pre-defined parameters

TABLE I

STRUCTURE AND MOTION PARAMETERS OF THE ROBOT

Symbols	Values	Definitions	
$[L_0, L_1, L_2]$	[0.045m,0.45m,0.4m]	length of links	structrue
d_2	0.057m	offset between the 1st-2nd joint	
$[W, L]$	[0.62m, 1.26m]	width and length of the trunk	
m	300Kg	mass of the trunk	
β	0.5	duty factor	motion
f	1.0Hz	gait frequency	

were obtained with the proposed method, as shown in Fig. 6. The error between the estimated values and the reference values maintained in the limits of 1cm.

The starting time 0ms in Fig. 6 corresponded to the moment when the swing legs completely left the ground in the first gait cycle. The disturbances during 0ms to 15ms existed because that at the beginning of the gait, the interaction between the standing feet and the ground was too complicated, and so were the feedback joint torques. So, the $p_{x,y}$ values during this period was not authentic. Before the leg phase exchange, the robot rotated about x_g-axis a little like an inverted pendulum. Since (12) used the assumption that $\{o_d\}$ and $\{o_g\}$ were parallel, this method was inaccuracy if the attitude angles deviated far from zero. So, only the data during the very primal period of the first gait (0ms $\sim$ 180ms) was accepted in this work. After this, the term ${}^{g}I$ would bring too much errors to the dynamic model.

Comparing to the public state-of-art methods, the main advantage of the proposed method is that it can identify the CoM position at the beginning of the dynamic trot gait without any pause of the robot motion. It will play a more important role when integrated with the robot attitude controller. In future works, the estimated CoM position will be used as a feedback state to optimize the motions of the

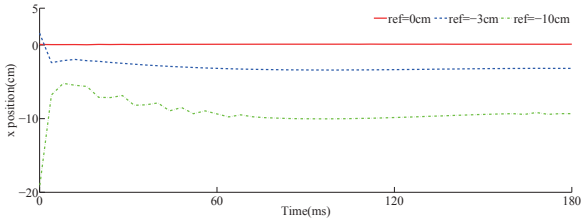

(a) The analytical xc position of CoM

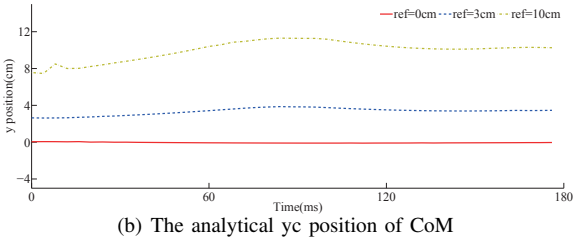

(b) The analytical yc position of CoM

Fig. 6. Simulation results of the CoM detection during the first half gait cycle

quadruped robot. The optimized motions will then maintain the robot orientation close to zero to make the proposed method practicable during the whole trot gait.

V. CONCLUSIONS

This work focused on the detection of the CoM position for quadruped robots in dynamic trot gait. The dynamic model of the robot trunk during trot gait was built in the inertial frame. Since the states of the robot were observed in the base frame, methods for transforming them to the inertial frame were provided. An analytical solution of the CoM position was obtained. To make the observations more precise, a step height compensation method was proposed to improve the motion performance of the robot. Two methods for obtaining the GRFs were compared and the more accurate one was adopted in this work. Simulation results showed the validity of the proposed method. Future works will focus on the reduction of the application of approximate calculations and will use the proposed CoM detection approach to optimize the motion controller.

REFERENCES

[1] M. Buehler, R. Playter, M. Raibert *et al.*, "Robots step outside," in *Int. Symp. Adaptive Motion of Animals and Machines (AMAM), Ilmenau, Germany*, 2005, pp. 1–4.

[2] G. Nelson, A. Saunders, and R. Playter, "The petman and atlas robots at boston dynamics," *Humanoid Robotics: A Reference*, pp. 169–186, 2019.

[3] S. Kuindersma, R. Deits, M. Fallon, A. Valenzuela, H. Dai, F. Permenter, T. Koolen, P. Marion, and R. Tedrake, "Optimization-based locomotion planning, estimation, and control design for the atlas humanoid robot," *Autonomous Robots*, vol. 40, no. 3, pp. 429–455, 2016.

[4] S. Y. Okita, V. Ng-Thow-Hing, and R. Sarvadevabhatla, "Learning together: Asimo developing an interactive learning partnership with children," in *RO-MAN 2009-The 18th IEEE International Symposium on Robot and Human Interactive Communication*. IEEE, 2009, pp. 1125–1130.

[5] P.-B. Wieber, R. Tedrake, and S. Kuindersma, "Modeling and control of legged robots," in *Springer handbook of robotics*. Springer, 2016, pp. 1203–1234.

[6] B. J. Stephens, "State estimation for force-controlled humanoid balance using simple models in the presence of modeling error," in *2011 IEEE International Conference on Robotics and Automation*. IEEE, 2011, pp. 3994–3999.

[7] J. Meng, Y.-b. Li, and B. Li, "Control method and its implementation of quadruped robot in omni-directional trotting gait," *Robot*, vol. 37, no. 1, pp. 74–84, 2015.

[8] T. Chen, X. Rong, Y. Li, C. Ding, H. Chai, and L. Zhou, "A compliant control method for robust trot motion of hydraulic actuated quadruped robot," *International Journal of Advanced Robotic Systems*, vol. 15, no. 6, pp. 1–16, 2018.

[9] S. Ma, T. Tomiyama, and H. Wada, "Omnidirectional static walking of a quadruped robot," *IEEE Transactions on Robotics*, vol. 21, no. 2, pp. 152–161, 2005.

[10] B. Chen, S. Li, and D. Huang, "Quadruped robot crawl gait planning based on dst," in *Proceedings of the 33rd Chinese Control Conference*. IEEE, 2014, pp. 8578–8582.

[11] M. Cognetti, P. Mohammadi, and G. Oriolo, "Whole-body motion planning for humanoids based on com movement primitives," in *2015 IEEE-RAS 15th International Conference on Humanoid Robots (Humanoids)*. IEEE, 2015, pp. 1090–1095.

[12] T. Horvat, K. Melo, and A. J. Ijspeert, "Model predictive control based framework for com control of a quadruped robot," in *2017 IEEE/RSJ International Conference on Intelligent Robots and Systems (IROS)*. IEEE, 2017, pp. 3372–3378.

[13] G. G. Muscolo, C. T. Recchiuto, C. Laschi, P. Dario, K. Hashimoto, and A. Takanishi, "A method for the calculation of the effective center of mass of humanoid robots," in *2011 11th IEEE-RAS International Conference on Humanoid Robots*. IEEE, 2011, pp. 371–376.

[14] H. Alai, F. A. Shirazi, and A. Yousefi-Koma, "New approach to center of mass estimation for humanoid robots based on sensor measurements and general lipm," in *2018 6th RSI International Conference on Robotics and Mechatronics (IcRoM)*. IEEE, 2018, pp. 388–393.

[15] S. Kwon and Y. Oh, "Estimation of the center of mass of humanoid robot," in *2007 International Conference on Control, Automation and Systems*. IEEE, 2007, pp. 2705–2709.

[16] M. Focchi, A. Del Prete, I. Havoutis, R. Featherstone, D. G. Caldwell, and C. Semini, "High-slope terrain locomotion for torque-controlled quadruped robots," *Autonomous Robots*, vol. 41, no. 1, pp. 259–272, 2017.

[17] G. Tournois, M. Focchi, A. Del Prete, R. Orsolino, D. G. Caldwell, and C. Semini, "Online payload identification for quadruped robots," in *2017 IEEE/RSJ International Conference on Intelligent Robots and Systems (IROS)*. IEEE, 2017, pp. 4889–4896.